ARTICLE NO. 79-0272R

J80-010

20002
20005

Optimal Nodal Point Distribution for Improved Accuracy in Computational Fluid Dynamics

Bion L. Pierson*
Iowa State University, Ames, Iowa
and
Paul Kutler†
NASA Ames Research Center, Moffett Field, Calif.

In applying finite-difference techniques to flowfield problems, the accuracy attained for a fixed number of node points can be improved using unequally-spaced node points. The distribution of these node points is chosen here by minimizing a measure of local truncation error with respect to the parameters which define a transformation between the computational space of equally-spaced node points and the physical space of unequally-spaced node points. The problem then becomes a nonlinear programming problem. Numerical results are presented for two one-dimensional test problems: the Blasius boundary-layer problem and the inviscid Burgers' equation.

I. Introduction

CURRENT computer speed and size limitations certainly encourage the development of more efficient flowfield analysis programs. In some cases, the problem is storage-bound, and the desired accuracy cannot be obtained due to an insufficiently fine mesh of nodal points. One of the most promising areas for obtaining substantial efficiency improvements in finite-difference methods is the use of nonuniformly-spaced nodal points. The primary objectives of this paper are to propose a simple, but systematic, means of redistributing nodal points for increased accuracy and to demonstrate with numerical examples the feasibility of its use.

Although there are several instances in which intuitive or heuristic "stretching" and "clustering" transformations have been used successfully in redistributing nodal points for better accuracy, very little research has been devoted to the development of systematic or optimal transformations. An interesting exception may be found in the paper by Gough et al.[1] in which a variational approach is applied to the problem of minimizing an indirect measure of the truncation error introduced by differencing. The resulting variational equations, which define the optimal transformation, are then solved along with the original flowfield (boundary-layer) equations by a standard finite-difference technique. One should also note that several attempts at grid optimization for finite-element methods are now underway as well.[2,3]

In contrast to Ref. 1, the approach taken here avoids the complications of a variational or optimal control approach and, in addition, allows for a direct measure of local truncation error to be minimized. The resulting problem is formulated as a nonlinear programming problem and is solved numerically. Accuracy comparisons are then made for numerical solutions obtained with and without the optimal transformations.

Presented as Paper 79-0272 at the AIAA 17th Aerospace Sciences Meeting, New Orleans, La., Jan. 15-17, 1979; submitted Jan. 29, 1979.

Index categories: Computational Methods; Boundary Layers and Convective Heat Transfer—Laminar.

*Professor, Dept. of Aerospace Engineering and the Engineering Research Institute. Associate Fellow AIAA.

†Research Scientist, Computational Fluid Dynamics Branch; currently with Flow Simulations, Inc., Sunnyvale, Calif. Associate Fellow AIAA.

II. Problem Formulation

The analysis and results presented here are restricted to one-dimensional spatial domains. Let the specified interval $[x_1,x_N]$ be partitioned by a nonuniform grid into $N-1$ subintervals $[x_i,x_{i+1}]$, $i=1,2,\ldots,N-1$, where N is fixed. Corresponding to the physical x-grid is a uniformly spaced computational ξ-grid which partitions the same interval into $N-1$ uniform subintervals $[\xi_i,\xi_i+h]$, $i=1,2,\ldots,N-1$, where $\xi_1=x_1$ and $h=(x_N-x_1)/(N-1)$. The x-grid is related to this ξ grid by the transformation $x=T(\xi)$.

Now, assume that the primary truncation error is introduced into the solution by estimating the flow variable spatial derivative $dE/d\xi$ using the second-order central difference equation

$$\frac{dE}{d\xi}=\frac{E[T(\xi_{i+1})]-E[T(\xi_{i-1})]}{2h} \tag{1}$$

Since the local truncation error associated with Eq. (1) is proportional to the third derivative, the performance index

$$J[T]=\frac{\delta}{2}\sum_{i=1}^{M-1}[(E_i''')^2+(E_{i+1}''')^2] \tag{2}$$

where $E_i'''\doteq d^3E[T(\xi)]/d\xi^3$ evaluated at $\xi=\xi_i$, is used. Equation (2) is simply a discrete approximation (trapezoidal rule) of the integral of E''' squared over the ξ domain. Since $E(x)$ is assumed to be available only in tabular form, 5-point symmetric difference equations

$$\delta^3E_1'''=-\frac{5}{2}E_1+9E_2-12E_3+7E_4-\frac{3}{2}E_5 \tag{3a}$$

$$\delta^3E_2'''=-\frac{3}{2}E_1+5E_2-6E_3+3E_4-\frac{1}{2}E_5 \tag{3b}$$

$$\delta^3E_i'''=-\frac{1}{2}E_{i-2}+E_{i-1}-E_{i+1}+\frac{1}{2}E_{i+2},\quad i=3,4,\ldots,M-2 \tag{3c}$$

$$\delta^3E_{M-1}'''=\frac{1}{2}E_{M-4}-3E_{M-3}+6E_{M-2}-5E_{M-1}+\frac{3}{2}E_M \tag{3d}$$

$$\delta^3E_M'''=\frac{3}{2}E_{M-4}-7E_{M-3}+12E_{M-2}-9E_{M-1}+\frac{5}{2}E_M \tag{3e}$$

coupled with polynomial interpolation of order k are used to estimate the E_i''' in Eq. (2). Here, $\delta=(x_N-x_1)/(M-1)$.

The transformation can be parameterized as follows:

$$x=T(\xi)=f(\xi,c)=\xi+(\xi-x_1)(x_N-\xi)\sum_{j=0}^{q-1}c_j\beta_j(\xi) \quad (4)$$

Chebyshev polynomials are used for the coordinate functions $\beta_j(\xi)$. The first five [0, 1]-shifted Chebyshev polynomials are given by

$$\beta_0=1$$

$$\beta_1=2\zeta-1$$

$$\beta_2=(8\zeta-8)\zeta+1$$

$$\beta_3=[(32\zeta-48)\zeta+18]\zeta-1$$

$$\beta_4=\{[(128\zeta-256)\zeta+160]\zeta-32\}\zeta+1 \quad (5)$$

where $\zeta=\xi/x_N$. Additional higher-order Chebyshev polynomials may be found in Table 3 of Ref. 4. For specified M, transformation order q, and polynomial interpolation order k, the performance index (2) now depends on the q-dimensional parameter vector $c=(c_0,c_1,\ldots,c_{q-1})^T$ and the flow variable table $E(x)$.

Finally, it is necessary to limit the spacing of the node points using an inequality constraint of the form

$$0<\epsilon\le f'(\xi,c)\le 1/\epsilon, \quad x_1\le\xi\le x_N, \quad 0<\epsilon<1 \quad (6)$$

where $f'=\partial f(\xi,c)/\partial\xi$ and ϵ is specified. These inequality constraints prevent extreme clustering or stretching of the x nodes. The x nodes will be clustered for $0<f'<1$ and stretched for $f'>1$. Note that a transformation satisfying Eq. (6) automatically satisfies the monotonicity constraint $f'\ge 0$ required for a one-to-one transformation.

The transformation selection problem can now be stated as a constrained parameter optimization problem: given an estimate of the solution $E(x)$, minimize a finite-difference approximation of Eq. (2) with respect to the elements of c, subject to the satisfaction of the parametric inequality constraint (6). The use of the transformation (4) has the advantage that this nonlinear programming problem is independent of the number of nodal points N. The null vector, which corresponds to the identity transformation, makes a convenient choice for the initial c vector. Since gradient information is not readily available, the direct search Nelder-Mead simplex method has been chosen for the optimization.[5] This method has a reputation for robust convergence characteristics on a wide range of problem types.

Penalty functions are used to enforce the inequality constraints (6). Unfortunately, these constraints depend on ξ in addition to the parameter vector c. Thus, each unconstrained subproblem is of the form

$$\min_c J_A(c)=J(c)+K\int_{x_1}^{x_N}F(\xi,c)\,d\xi \quad (7)$$

where

$$F(\xi,c)=(\epsilon-f')^2H(\epsilon-f')+\left(f'-\frac{1}{\epsilon}\right)^2H\left(f'-\frac{1}{\epsilon}\right) \quad (8)$$

$$H(\alpha)=\begin{cases}1, & \alpha>0\\ 0, & \alpha\le 0\end{cases} \quad (9)$$

and the integral in Eq. (7) is evaluated by trapezoidal rule based on L uniform intervals. The function $f'(\xi,c)$ can be readily derived analytically from Eqs. (4) and (5). In practice, it has proven satisfactory to choose K sufficiently large so that J_A-J serves as a "barrier" function for which a single unconstrained subproblem (7) provides a good estimate of the actual constrained minimum.

For the special case $q=1$, one can readily obtain explicit bounds on c which ensure satisfaction of Eq. (6). In this case, the derivative function f' is linear in ξ:

$$f'(\xi,c)=c_0(x_1+x_N)+1-2c_0\xi \quad (10)$$

Note that $f'[(x_1+x_N)/2,c_0]=f'(\xi,0)=1$ for all $x_1\le\xi\le x_N$ and all finite c_0. Therefore, the straight line Eq. (10) simply rotates about the point $(f',\xi)=[1,(x_1+x_N)/2]$ as c_0 is varied. Since $1-\epsilon<\epsilon^{-1}-1$, the lower bound constraint, $f'\ge\epsilon$, always becomes active first for deviations of c_0 from zero. The limits on c_0 for which Eq. (6) are satisfied are given by

$$|c_0|\le(1-\epsilon)/(x_N-x_1) \quad (11)$$

For $q=1$, it becomes convenient to use a golden section search in minimizing J over the interval of Eq. (11). But, in general for $q>1$, it becomes necessary to rely on a penalty function enforcement of Eq. (6) based on a large number of f' calculations as explained above.

III. Numerical Examples

All computations have been performed on the Iowa State University Computer Center's coupled IBM 360/65 and Itel AS/5 computers using a FORTRAN IV compiler and double precision arithmetic. The algorithm used for the Nelder-Mead simplex method is a slightly modified version of that presented by O'Neill.[6] The minimization process is terminated whenever the variance of the $q+1$ function values corresponding to the vertices of the current simplex becomes less than a user-specified termination tolerance, say ϵ_{NM}.

Blasius Boundary-Layer Problem

The equations of motion for two-dimensional incompressible laminar flow over a flat plate parallel to the free stream may be written as

$$u\frac{\partial u}{\partial X}+v\frac{\partial u}{\partial Y}=\nu\frac{\partial^2 u}{\partial Y^2} \quad \text{(momentum)} \quad (12a)$$

$$\frac{\partial u}{\partial X}+\frac{\partial v}{\partial Y}=0 \quad \text{(continuity)} \quad (12b)$$

with boundary conditions:

$$\begin{cases}u(X,0)=v(X,0)=0\\ u(X,\infty)=U_\infty\end{cases} \quad (12c)$$

The similarity transformation

$$\eta=X$$

$$x=Y[U_\infty/(\nu X)]^{1/2} \quad (13)$$

is then applied to Eqs. (12). For our immediate purposes, the primary advantage in applying Eqs. (13) is to provide a steady-state solution which is independent of the longitudinal coordinate η (marching direction). Thus, only the transverse nodal points need to be redistributed according to transformation (4). The optimization and subsequent accuracy comparisons are based only on the horizontal velocity component so that, in our previous notation, $E=u$. Euler-implicit differencing has been used. The system of linear equations resulting from the finite-difference approximations is solved by tridiagonal elimination.

The problem is first solved with N equally-spaced nodal points. The constant data, $x_1=0$, $x_N=8$, $U_\infty=30.48$ m/s (100 ft/s) and $\nu=1.486\,(10^{-3})$ m^2/s [1.6 (10^{-4}) ft^2/s], are used

throughout. Based on this solution, an optimal transformation is obtained for specified values of q,k,M, and ϵ_{NM} as described in Sec. II. Then, a second solution is obtained using this optimal transformation. Finally, for comparison purposes, the problem is solved a third time with $2N-1$ equally-spaced nodal points. Thus, a solution using an optimal transformation based on the results for N equally-spaced nodal points is compared for accuracy both with the original solution and with a solution using twice as many uniform grid intervals. The scalar measure of accuracy for each solution is defined as the root-mean-square error between the 40 solution points given by Schlichting[7] and the interpolated values obtained from the numerical solution in question. The entire process of obtaining three comparison solutions can, of course, be repeated for different N,q,k, and M values.

Almost all numerical solutions to the Blasius problem are qualitatively correct, and it becomes difficult to readily distinguish solution points on a graph. For illustrative purposes, therefore, a pair of very coarse grid $N=7$ solutions are shown along with the exact solution in Fig. 1. In this case the use of an optimal transformation provides a 65.9% reduction in the error measure. This compares with a 75.7% error measure reduction when using 13 uniformly-spaced nodal points instead. For a broad range of ϵ values, the constraints (6) are not binding on the optimal transformation for this problem and therefore are not enforced.

A set of solutions for $N=15$ was obtained for various interpolation orders. The results are listed in Table 1 and indicate that it is important, especially for small N, to use a sufficiently high order interpolation since finite differences are being used to estimate E'''. However, for $k\geq 3$, the final results do not differ appreciably. Plots of E''' with and without the optimal transformation for the $k=7$ case are shown in Fig. 2. The corresponding velocity profiles are presented in Fig. 3, and the optimal transformation and its slope history are shown in Figs. 4 and 5, respectively.

Finally, a comparison of transformation orders is presented in Table 1 for the case of $N=41$. Clearly, for this problem, relatively good accuracy gains can be achieved for q as low as 3.

Inviscid Burgers' Equation: Backward Step Initial Conditions

As a second test problem exhibiting a steady-state solution, the inviscid Burgers' equation[8] with backward step initial conditions is considered next.

$$\frac{\partial u}{\partial t}+u\frac{\partial u}{\partial x}=0 \tag{14}$$

$$u(x,0)=\begin{cases}1, & 0\leq x<0.5\\ 0, & x=0.5\\ -1, & 0.5<x\leq 1\end{cases} \tag{15}$$

Table 1 Solution accuracy for the Blasius boundary-layer problem

N	q	k	M	ϵ_{NM}	PEMR/OT[a]	PEMR/D[b]
7	8	3	41	10^{-14}	65.9	75.7
15	8	1	61	10^{-10}	−14.1	75.2
15	8	2	61	10^{-10}	36.6	75.2
15	8	3	61	10^{-10}	66.6	75.2
15	8	6	61	10^{-14}	72.5	75.2
15	8	7	61	10^{-14}	76.6	75.2
41	3	5	51	10^{-17}	72.5	75.3
41	5	5	51	10^{-17}	77.6	75.3
41	8	5	51	10^{-17}	80.6	75.3

[a] Per cent error measure reduction: solution using an optimal transformation compared to that for equally-spaced nodal points. [b] Per cent error measure reduction: solution with $2N-1$ equally-spaced nodal points compared to that with N equally-spaced nodal points.

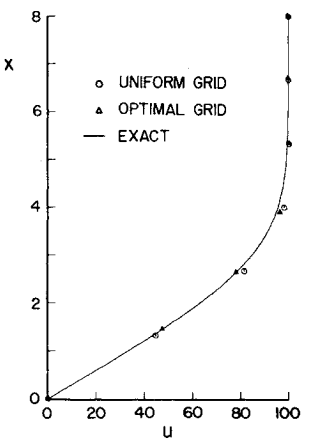

Fig. 1 Velocity profile for the Blasius problem: $N=7$, $q=8$, $k=3$, $M=41$, $\epsilon_{NM}=10^{-14}$.

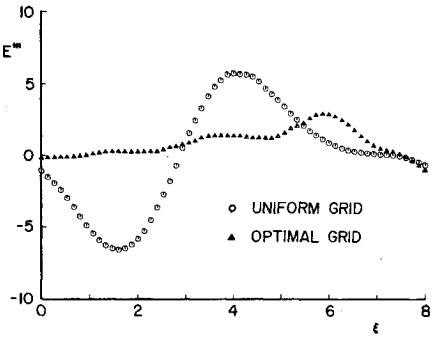

Fig. 2 Third derivative estimate with and without an optimal transformation: Blasius problem, $N=5$, $q=8$, $k=7$, $M=61$, $\epsilon_{NM}=10^{-14}$.

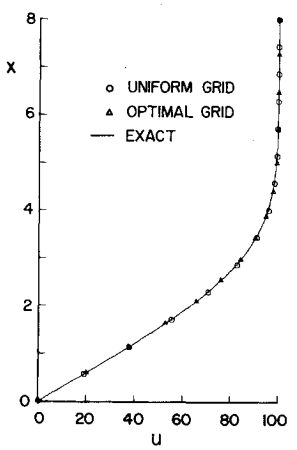

Fig. 3 Velocity profile for the Blasius problem: $N=15$, $q=8$, $k=7$, $M=61$, $\epsilon_{NM}=10^{-14}$.

When transformed via $\tau=t$ and $\xi=\xi(x)$, Eq. (14) becomes

$$\frac{\partial U}{\partial \tau}+\frac{\partial E}{\partial \xi}=0 \tag{16}$$

where $U=u/(\partial\xi/\partial x)$ and $E=\frac{1}{2}u^2$. Equation (16) is in strong conservation law form and will be solved numerically using the noniterative implicit method of Beam and Warming.[9] Euler-implicit differencing is used for the time differencing, and the spatial differencing is done by second-order central differences. A Courant number of 1.0 and a dissipative coefficient of 1.0 for the added fourth-order dissipative term have been used throughout. In each case, a steady-state solution is defined as that solution obtained after 100 time steps of 0.0025-s duration each. The accuracy of a given solution is computed as a 50-point rms of the differences between interpolated solution points and Eq. (15) over the half interval $0\leq x\leq 0.5$.

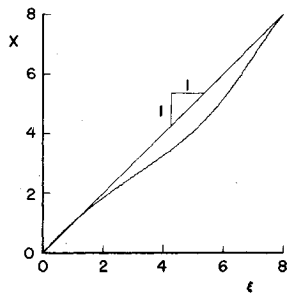

Fig. 4 Optimal transformation for the Blasius problem: $N=15$, $q=8$, $k=7$, $M=61$, $\epsilon_{NM}=10^{-14}$.

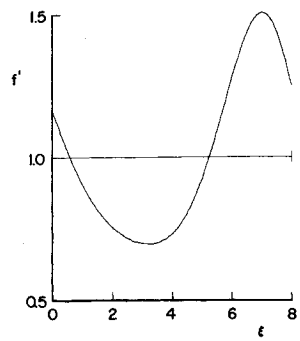

Fig. 5 Optimal transformation slope history for the Blasius problem: $N=15$, $q=8$, $k=7$, $M=61$, $\epsilon_{NM}=10^{-14}$.

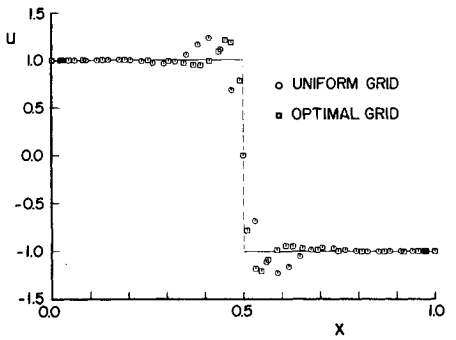

Fig. 6 Solution to Burgers' equations with backward step initial conditions: $N=M=35$, $q=12$, $k=7$, $\epsilon=0.1$.

Anticipating the obvious midpoint symmetry present in the solutions, a symmetric transformation of the form

$$f(\xi,c)=\xi[1+(0.5-\xi)\sum_{j=0}^{q-1}c_j\beta_j(\zeta_1)],0\le\xi\le0.5$$

$$f(\xi,c)=\xi-(1-\xi)(\xi-0.5)\sum_{j=0}^{q-1}c_j\beta_j(\zeta_2),0.5\le\xi\le1 \qquad (17)$$

where $\zeta_1=2\xi$ and $\zeta_2=2(1-\xi)$ is used for this problem. Again, a numerical solution is first obtained for N equally-spaced nodal points. An optimal transformation (17) is then computed for the $E(x)$ table just obtained, and a second solution is obtained for N optimally-spaced nodal points. Several results are listed in Table 2. Solutions for $N=35$ with and without an optimal transformation are shown in Fig. 6. The solution with optimal nodal point distribution is clearly superior and in fact yields a 55.7% reduction in the solution error measure. This accuracy gain exceeds that obtained by simply doubling the number of uniformly-spaced grid intervals. This $N=35$ optimal transformation is presented in Fig. 7. The slope history for that same transformation is given in Fig. 8. Note that the primary clustering takes place near the midpoint ($\xi=0.5$) where the extreme gradients are encountered.

Better relative performance can be obtained for larger N since a more accurate $E(x)$ table is then available for use in optimizing the transformation. As an illustration, results for $N=51$, $q=12$ are shown in Table 2 and may be compared with those already presented for $N=35$. Finally, a set of results for $N=51$ and $q=8$ (also shown in Table 2) indicates that it may be unnecessary to use $q>8$ for satisfactory accuracy gains.

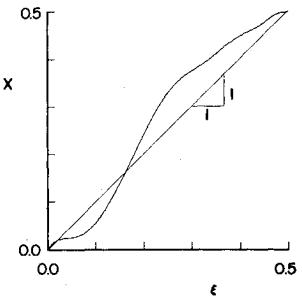

Fig. 7 Optimal transformation for the Burgers' equation problem with backward step initial conditions: $N=M=35$, $q=12$, $k=7$, $\epsilon=0.1$.

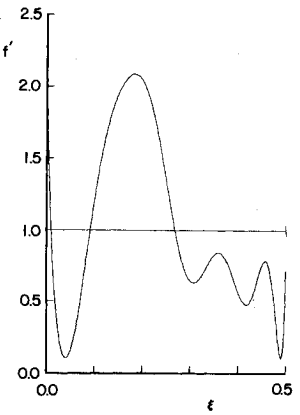

Fig. 8 Optimal transformation slope history for the Burgers' equation problem with backward step initial conditions: $N=M=35$, $q=12$, $k=7$, $\epsilon=0.1$.

Inviscid Burgers' Equation: Sinusoidal Initial Conditions

To demonstrate that this approach can be beneficial on problems with time-varying solutions as well, the inviscid Burgers' equation (14) will be treated again. This time the initial condition will be

$$u(x,0)=\sin(2\pi x),\quad 0\le x\le1 \qquad (18)$$

In this case, the solution envolves to a sharp standing "N wave" in approximately 0.25 s and subsequently attenuates slowly toward a uniform zero solution. The various solutions will be compared for accuracy at $t=0.25$ s and will all be computed on the basis of 50 uniform time steps with a time increment of 0.005. The measure of accuracy is a 50-point rms error over the half interval $0\le x\le0.5$ based on an "exemplar" solution obtained with $N=501$.

The optimal transformation is first computed on the basis of $E=\frac{1}{2}u^2$ and Eq. (18). After a fixed number of time steps, the finite-difference process is interrupted while a new or

Table 2 Solution accuracy for the inviscid Burgers' equation with backward step initial conditions: $M=N$, $k=7$, $\epsilon=0.1$

N	q	PEMR/OT[a]	PEMR/D[b]
35	12	55.7	50.6
51	12	72.2	64.3
51	8	67.2	64.3
51	1	62.7	64.3

[a] Per cent error measure reduction: solution using an optimal transformation compared to that for equally-spaced nodal points. [b] Per cent error measure reduction: solution with $2N-1$ equally-spaced nodal points compared to that with N equally-spaced nodal points.

Table 3 Solution accuracy for the inviscid Burgers' equation with sinusoidal initial conditions: $N=M=41$, $q=12$, $k=7$, PEMR/D[b] = 58.3

Number of sequential transformation optimizations	ϵ	PEMR/OT[a]
2	0.2	23.1
5	0.2	78.0
5	0.5	46.6
5	0.1	40.0

[a]Per cent error measure reduction: solution using an optimal transformation compared to that for equally-spaced nodal points. [b]Per cent error measure reduction: solution with $2N-1$ equally-spaced nodal points compared to that with N equally-spaced nodal points.

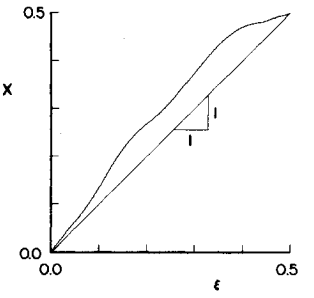

Fig. 9 Optimal transformation for the Burgers' equation problem with sinusoidal initial conditions: Fifth optimization at $t=0.2$, $N=M=41$, $q=12$, $k=7$, $\epsilon=0.2$.

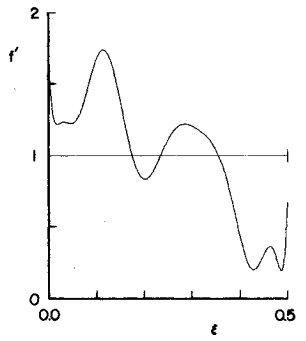

Fig. 10 Optimal transformation slope history for the Burgers' equation problem with sinusoidal initial conditions: Fifth optimization at $t=0.2$, $N=M=41$, $q=12$, $k=7$, $\epsilon=0.2$.

updated optimal transformation is computed on the basis of the current $E(x)$. By periodically recomputing the optimal transformation, one hopes to provide the finite-difference process with a transformation (piecewise-constant in time), which is approximately optimal for all t. Of course, with each new optimal transformation it becomes necessary to recompute by interpolation new u values corresponding to the new x-points before resuming the finite-difference solution process. The solution obtained using N nodal points and periodically updated optimal transformations is then compared for accuracy with solutions for both N and $2N-1$ uniformly-spaced nodal points.

Results are listed in Table 3 for both 2 and 5 periodic transformation optimizations. As expected, a dramatic increase in accuracy is achieved in the latter case for more frequent updating of the transformation. For the case of 5 transformation updates, note that it is disadvantageous to allow extreme clustering (small ϵ) since a "finely-tuned" optimal transformation at one time instant becomes a rather poor transformation for other times. The optimal transformation and corresponding slope history for the case of $N=41$, $q=12$, $\epsilon=0.2$, and the 5th (and last) transformation update are presented in Figs. 9 and 10, respectively. This transformation is based on the almost fully-developed N-wave.

IV. Conclusions and Discussion

Several conclusions emerge from the results obtained thus far:

1) Transformations which minimize a measure of local truncation error do in fact provide significant accuracy improvement in the final solution.

2) The use of an optimal transformation for problems with steady-state solutions can provide at least as much error reduction as can doubling the number of uniform intervals.

3) Similar error reduction is available for time-varying solutions with strong gradients if the optimal transformation is recomputed periodically to "follow" the solution.

4) For time-varying solutions, it becomes advantageous to use "moderate" optimal transformations based on an f' constraint bound ϵ which is not too small and a relatively large termination tolerance ϵ_{NM}.

5) Useful optimal transformations can be obtained with relatively few transformation parameters ($3 \le q \le 8$).

It is difficult to make sharp predictions of the best choices for q,k,ϵ, and other user-specified parameters simply because the minimum measure of local truncation error does not coincide with the minimum solution error measure. In general, the "optimal" transformation [which minimizes Eq. (2)] will be only suboptimal with respect to ultimate solution accuracy, though it will provide substantial accuracy gains. It appears that one is more likely to "over-optimize" for small N.

One must exercise care in choosing the interpolation order. Poor interpolation will result in inaccurate finite-difference estimates of E'''. In fact, it is a good idea to obtain computer plots of E''' for various k values and check for relative smoothness. For N small, a relative large k may be required. But, for moderate to large N values, any moderate interpolation order ($3 \le k \le 7$) appears to provide nearly the same final results.

The relative cost of obtaining an optimal transformation, in the sense defined here, is not negligible. However, once an optimal transformation has been obtained from one solution estimate, it may be used as a suboptimal transformation for related problems (parametric studies) and/or refined with little additional cost once a better solution is available. It should not be necessary to always use the very "best" optimal transformation.

Although the optimization techniques used here are not new, the application is. The approach presented here has been successfully demonstrated on several one-dimensional test problems and gives promise of significant accuracy gains for more difficult problems.

Acknowledgments

This work was supported by the Engineering Research Institute of Iowa State University, Ames, Iowa, through funds provided by the NASA Ames Research Center under Grant NCA2-OR340-705. The authors would like to express their appreciation to S. R. Chakravarthy for providing the basic finite-difference codes used in the numerical examples.

References

[1]Gough, D. O., Spiegel, E. A., and Toomre, J., "Highly Stretched Meshes as Functionals of Solutions," *Proceedings of the 4th International Conference on Numerical Methods in Fluid Dynamics*, edited by R. D. Richtmyer, *Lecture Notes in Physics*, Vol. 35, Springer-Verlag, New York, 1975, pp. 191-196.

[2]Tang, J. W. and Turcke, D. J., "Characteristics of Optimal Grids," *Computer Methods in Applied Mechanics and Engineering*, Vol. 11, April 1977, pp. 31-37.

[3]Felippa, C. A., "Numerical Experiments in Finite Element Grid Optimization by Direct Energy Search," *Applied Mathematical Modelling*, Vol. 1, June 1977, pp. 239-244.

[4] *Tables of Chebyshev Polynomials* $S_n(x)$ *and* $C_n(x)$, U.S. National Bureau of Standards, Applied Mathematics Series, No. 9, 1952.

[5] Nelder, J. A. and Mead, R., "A Simplex Method for Function Minimization," *Computer Journal*, Vol. 7, Jan. 1965, pp. 308-313.

[6] O'Neill, R., "Algorithm AS 47. Function Minimization Using a Simplex Procedure," *Applied Statistics*, Vol. 20, No. 3, 1971, pp. 338-345.

[7] Schlichting, H., *Boundary-Layer Theory*, 6th ed., McGraw-Hill Book Co., New York, 1968, p. 129.

[8] Burgers, J. M., *The Nonlinear Diffusion Equation*, D. Reidel Publishing Co., Dordrecht, Holland, 1974, p. 9.

[9] Beam, R. M. and Warming, R. F., "An Implicit Factored Scheme for the Compressible Navier-Stokes Equations," *AIAA Journal*, Vol. 16, April 1978, pp. 393-402.